Hindawi Publishing Corporation
ISRN Forestry
Volume 2013, Article ID 485264, 8 pages
http://dx.doi.org/10.1155/2013/485264

Research Article

Using Multispectral Spaceborne Imagery to Assess Mean Tree Height in a Dryland Plantation

Michael Sprintsin,[1,2] Pedro Berliner,[1] Shabtai Cohen,[3] and Arnon Karnieli[1]

[1] *Jacob Blaustein Institutes for Desert Research, Ben-Gurion University of The Negev, 84990 Sede Boqer Campus, Israel*
[2] *Forest Management and GIS Department, Land Development Authority, Forest Department, Jewish National Fund (KKL), Eshtaol, M.P., 99775 Shimshon, Israel*
[3] *Institute of Soil, Water and Environmental Sciences, Agricultural Research Organization, The Volcani Center, 50250 Bet Dagan, Israel*

Correspondence should be addressed to Michael Sprintsin; michaelsp@kkl.org.il

Received 11 April 2013; Accepted 9 May 2013

Academic Editors: M. Kanashiro and H. Zeng

This study presents an approach for low-cost mapping of tree heights at the landscape level. The proposed method integrates parameters related to landscape (slope, orientation, and topographic height), tree size (crown diameter), and competition (crown competition factor and age), and determines the mean stand tree height as a function of tree competitive capability. The model was calibrated and validated against a standard inventory dataset collected over a dryland planted forest in the eastern Mediterranean region. The validation of the model shows a high and significant level of correlation between measured and modeled datasets ($R^2 = 0.86$; $P < 0.01$), with almost negligible (less than 1 m) levels of absolute and relative errors. The validated model was implemented for mapping mean tree height on a per-pixel basis by using high-spatial-resolution satellite imagery. The resulting map was, in turn, validated against an independent dataset of ground measurements. The presented approach could help to reduce the need for fieldwork in compiling single-tree-based inventories and to apply surface-roughness properties to hydrometeorological studies and regional energy/water-balance evaluation.

1. Introduction

Tree height is considered to be a useful structural variable in estimating wood volumes, biomass, carbon stocks, and productivity of forest stands. It also determines the light penetration into the forest canopy and is of importance for certain habitat studies. In addition, tree height plays an essential role in micrometeorological research and global climate modeling by determining forest aerodynamic roughness (i.e., zero-plane displacement and roughness length) and affecting the transport of energy and substances between the land surface and the atmosphere boundary layer [1]. Therefore, the computation and mapping of tree-height distribution in a widespread area becomes a key step in characterizing the land-surface physical processes.

Although the relationship between vegetation structure and surface reflectance obtained from satellite observation has been a focus of a great deal of research, the evaluation of mean tree height is still one of the main challenges for remote sensing applications. The most frequently used remote sensing techniques that are relevant to evaluation of tree height are (1) automated photogrammetry (e.g., [2]); (2) airborne ranging radar (e.g., [3]); and (3) laser altimetry (e.g., [4–6]). Since these methods are mainly based on airborne platforms, the data collected by them is naturally of high resolution, and usually enables observation of an individual tree within a stand. Though such data are accurate and therefore attractive for use, they are still very expensive to obtain. Thus, for operational use and for covering relatively large territories, it is more convenient to use low-cost high-frequency observations at lower spatial resolution, such as those obtained from passive optical systems (e.g., [7, 8]). However, the imagery obtained by such sensors presents significant limitations for forestry applications, because not every forest parameter has its own unique spectral response. Thus, for large-area studies, the spectral vegetation index

approach, that is, a single value generated by combining data from multiple spectral bands, seems to be more appropriate.

The most basic spatial variable of the land surface that can be simply extracted from optical remote sensing data is the canopy cover (CC). From the ecological point of view, CC is an important parameter of a forest ecosystem for it is related to species richness and wildlife habitat and behavior (e.g., [9]); also, it is significant in studies of natural-hazard dynamics and understory vegetation productivity [10]. Technically, it can be assessed either by linear normalization of spectral vegetation indices [11, 12] or by supervised or unsupervised classification of multispectral imagery [13]. Both procedures are relatively simple and easily applied by users with varied levels of training. Furthermore, correlation of CC with other stand parameters could be straightforward, according to allometric relationships. It should be remembered, however, that, theoretically, the same level of CC could be found in dense stands of small trees and sparse stands of tall trees. Although in practice such similarity is unlikely to be found, the possibility highlights that CC could not be taken either as a unique or as a "stand-alone" predictor of mean tree height in the stand, and more robust combination of variables is required. Nevertheless, we assumed that stand-level canopy cover, as deduced from multispectral remote sensing imagery, can be used as a proxy for those variables, and our objective was to test this assumption in order to map mean tree height distribution on the landscape scale.

Although the majority of remote sensing applications for forestry cover a wide variety of ecoregions (e.g., [14]), the implementation of such techniques in predominantly water-limited ecosystems has rarely been reported being a subject only of some recent developments (e.g., [15–17]). However, such ecosystems occupy a significant part of the Earth's surface and are continually afforested. Because of the particular environmental problems common in such environments (e.g., low rainfall concentrated in short periods during the year, poor and shallow soils, high temperatures, and low relative humidity) and the relatively simple vegetation structure associated with these problems, landscape-level modeling is necessary to predict and optimize the benefits dryland forestry can contribute to ecosystem sustainability. Therefore, the development of applications that can be easily implemented in drylands is important from both ecological and silvicultural points of view. All in all, the major justification and motivation for our present study is specifically addressing the applicability of remote sensing in studying the structure of dryland planted forest that can be deemed as being typical of large tracts of afforested lands of the eastern Mediterranean. This assumes that little information is available and that little testing has been done until now.

The presented approach is based on a standard inventory dataset that was divided into calibration and validation data subsets. The former was used for choosing independent variables and calculating required coefficients; the latter was used for model validation. The validated model was then implemented for mapping mean tree height on a per-pixel basis, by means of multispectral high-spatial-resolution satellite imagery. The resulting map was, in turn, validated against an independent dataset of ground-based measurements.

This paper is structured as follows: first, the modeling approach is presented, then the validation data subset is analyzed, and finally, mean tree height distribution is mapped and validated within a specific studied area.

2. Theoretical Model

Although, the height to which trees can grow is still poorly understood, it is a common assumption that it is primarily limited by hydraulic factors, that is, by the tree's ability to transport water from roots to top. Consequently, Koch et al. [18] stated the following: "trees grow tall where resources are abundant, stresses are minor, and competition for light places a premium on height growth." Therefore, in water-limited environments mean tree height can be presented as a function of a tree's competitive abilities. These abilities reflect the interaction of any tree in a specific stand with other surrounding individuals (e.g., [19]) and to some extent are determined by landscape characteristics. The latter determine the water redistribution within a specific area and control the interception of incoming solar radiation.

Accordingly, we present mean tree height (H_t) as a variable related to competition (COMP) and landscape (i.e., site) factors (SITE):

$$H_t = a + (b \times \mathrm{COMP}) + (c \times \mathrm{SITE}), \quad (1)$$

where COMP reflects characteristics of an individual tree and its behavior within a specific stand, SITE is related to specific plot elevation and orientation, and a, b, and c are regression coefficients.

Although the relationship between those factors is not necessarily linear, that is, of the form of (1), the lack of attention to this problem in the current literature allows us to test the applicability of this simplified intuitive approximation to exploration of the relationship between H_t and other stand variables. Moreover, many existing approaches that examine the dependency of any target stand characteristic on the combined effect of ecophysiological factors use linear relationships (e.g., [20, 21]) which support the assumption that (1) can serve as a reasonable approximation for H_t.

Since our major concern was the ability to evaluate H_t on the landscape level, in order to solve (1) we included in the final formulation only variables that were accessible—directly or indirectly—via remote sensing imagery or from existing databases. Those variables were carefully selected from the calibration data subset that initially included the entire set of inventory measures: age, diameter at breast height, tree and plot basal area, crown width, soil depth, and number of trees per plot (TPP).

Competition (COMP) has been defined as a parameter that depends on the maturity of a particular stand and involves the within-stand interaction between individuals. To characterize such relationships, we considered the crown competition factor (CCF; [22]) and stand age as independent predictors of "COMP."

The advantage of using CCF, which represents the area available to the average tree in the stand in relation to the

Table 1: Comparative statistics for calibration and validation data subsets.

Parameter	Calibration subset			Validation subset		
	Range	Average	STD	Range	Average	STD
H_t (m)	5–10	8	1	4–11	9	2
DBH (m)	0.12–0.2	0.16	0.02	0.10–0.19	0.16	0.03
CW (m)	3–5	4	1	3–5	4	1
CC (%)	25–91	56	20	28–90	56	19
TPP	6–10	7	1	7–10	8	2
Age (years)	32–37	35	1.5	30–38	35	2.3

H_t represents mean tree height; DBH: diameter at breast height; CW: crown width; CC: canopy cover, TPP number of trees per plot, and STD: standard deviation.

maximum area it could use if it existed in isolation [23], is that it is generally independent of site and age. A logarithmic transformation of CCF was used to reduce the effect of sampling variation in large estimates of CCF [20].

There are very few published studies of the impact of stand age and competition on simple measures of tree size. However, the age-related decline in productivity and biomass development of forests after canopy closure is well known and well documented (e.g., [24–28]). Therefore, we assume that the reason for such a decline is age-related decrease in tree competitive abilities, in which case, one would expect that any combined effect of age and CCF (that implies the influence of CC) would be representative as a measure of competition:

$$b \times \mathrm{COMP} = b_1 + [b_2 \times \ln(\mathrm{CCF})] + [b_3 \times \mathrm{Age}]. \quad (2)$$

The "SITE" factors are plot-specific variables that characterize the topography and the orientation of a plot. They were computed after Hasenauer and Monserud [20] as

$$\begin{aligned} d \times \mathrm{SITE} = {} & [d_1 \times \mathrm{ELEV}] + [d_2 \times \mathrm{ELEV}^2] + [d_3 \times \mathrm{SL}] \\ & + [d_4 \times \mathrm{SL}]^2 + [d_5 \times \mathrm{SL} \times \sin(\mathrm{AS})] \\ & + [d_6 \times \mathrm{SL} \times \cos(\mathrm{AS})], \end{aligned} \quad (3)$$

where ELEV is the elevation of the site (m), SL is the slope (°), and AS is the aspect (i.e., the direction in which a slope faces) that were calculated from the digital terrain model (DTM; [29]).

3. Materials and Methods

3.1. Study Area. The study was conducted in the Yatir forest (31°35′ N and 35°05′ E, 630 m AMSL; area ~3000 ha) located in a transitional area between arid and semiarid climatic zones in southern Israel. The long-term average annual precipitation is ~285 mm, and the average total annual potential evapotranspiration is 1600 mm. The forest comprises predominantly of *Pinus halepensis* Mill. trees, mostly planted during 1964–1974. Average tree density is ~320 ± 75 trees ha^{-1} [17], mean tree height (H_t) ~9 ± 2 m, diameter at breast height (DBH) ~17 ± 4 cm, canopy cover (CC) ~53% ± 15%, and effective leaf area index (LAI) ~1.7 [30]. The trees grow on shallow Rendzina and lithosol soils, 0.2–1.5 m in depth that overlay chalks and limestone. The understory vegetation develops during the rainy season and disappears shortly thereafter [31]. The specific study area (SSA) was set to 1 km^2 at the central most mature part of the forest, which was planted in the late 1960 s.

3.2. Sampling Design, Measurements, and Calculations. The Israeli Forest Service provided the inventory dataset. The data collection followed the traditional line-plot cruising approach, with circular plot shape [23]. Ninety-seven plots, each of 200 m^2, were established throughout the studied forest by using a forest map overlaid with the network of 250 m^2 quadrates. Training plots were located at the upper right-hand corner of every second quadrate. On each tree located within each training plot, we measured (a) DBH (measured with a caliper 1.37 m above the ground); (b) crown width (CW; measured with a measuring tape as the average of four different diameters of the canopy extension as observed from below); and (c) H_t (measured with a clinometer). Plot basal area was calculated from DBH measurements. The tree canopy was assumed to be circular, and CW that represented an equivalent canopy diameter was used to compute the crown area (CA). Canopy cover (CC) was calculated as the ratio of the sum of the crown area of all trees within a plot to the area of the plot, as adjusted for canopy overlap, according to Crookstone and Stage [32].

The entire set of 97 plots was then arbitrarily separated into calibration and validation subsets, comprising, respectively, 73 and 24 plots, that is, ~75% and ~25%, respectively, of all the plots. Both subsets were chosen with the aid of a random number generator [33, 34]. Comparative statistics for both subsets are presented in Table 1. Each subset has been classified into 5% CC classes. The mean value of each measured and calculated variable was estimated per CC class.

In addition, an independent dataset of measurements was collected over the six 1000 m^2 plots chosen within a specific research site of about 1 km^2. The exact spatial location and the perimeter of each plot were determined with a GPS (GPS) receiver with an accuracy of ±2 m. The results were then converted into a GIS polygon vector layer by using the MapInfo Professional software, Version 7.0. This additional dataset was used to validate a map of mean tree height prepared by using multispectral satellite imagery.

3.3. Multicollinearity Test. As we stated above, CCF is an age-independent parameter. However, some degree of multicollinearity between age and CCF still might be expected, because the studied forest is subject to intensive management practice that aims to reduce tree density as age increases, to provide optimal growing conditions for the remaining trees. Although there is no statistical test that can determine whether or not multicollinearity is a problem [35], its extent can be detected via the variance inflation factor (VIF; [36]) which measures the impact of multicollinearity among the predictors on the precision of estimation. The VIF is computed as $(1/(1 - R^2))$ for each independent variable. A general rule is that VIF higher than 10 indicates problems with multicollinearity [37, 38], that is, that the correlation between certain predictor variables is so large that they do not provide adequately independent information for reliable predictions.

3.4. Satellite Data Acquisition and Processing. A multispectral IKONOS image obtained on March 21, 2004 under cloud-free sky conditions was used. IKONOS has four spectral bands in the blue (0.45–0.52 μm), green (0.51–0.60 μm), red (0.63–0.70 μm), and near-infrared (0.76–0.85 μm) regions. An IKONOS image covers a nominal area of 16 km × 16 km at nadir with a spatial resolution of 4 m in all multispectral bands. The image was radiometrically and atmospherically corrected according to supplier's instructions (http://www.geoeye.com/products/imagery/ikonos/spectral.htm) and the 6S radiative transfer model [39] and registered into the UTM projection by using 20 ground control points (GCPs) obtained in the field with the dGPS receiver, resulting in average rectification errors of 0.7 and 0.85 pixels for the X and Y planes, respectively. The SSA was then extracted from the entire image with the ERDAS Imagine software.

The degree of canopy cover for an independent six-plot dataset has been described in terms of fractional vegetation cover (FVC). For that we used a simplified two-end member spectral mixture analysis model comprising a single equation that presents a surface reflectance measured by a satellite as the weighted sum of canopy and background reflectance terms [11, 30]. These two terms are further represented by minimum (min) and maximum (max) values of the normalized difference vegetation index (NDVI), obtained from in-situ reflectance measurements carried with a LICOR LI-1800 high-spectral-resolution field spectroradiometer, operating in the range 400–1100 nm with spectral resolution of 2 nm, yielding

$$\mathrm{FVC} = \left(\frac{\mathrm{NDVI} - \mathrm{NDVI}_{\min}}{\mathrm{NDVI}_{\max} - \mathrm{NDVI}_{\min}}\right)^{0.645}. \quad (4)$$

The FVC was then compared with the CC, as calculated from field measurements.

4. Results

4.1. Variance Inflation Factor and Multicollinearity. The statistical analysis did not support the expectation of multicollinearity between age and ln(CCF) measures; it yielded a VIF value of 1.15. In addition, the direct comparison between the two variables, which resulted in a very weak and insignificant linear correlation ($R^2 = 0.13$; $P = 0.28$), also served as a supplementary proof for the lack of multicollinearity between parameters used to represent competition.

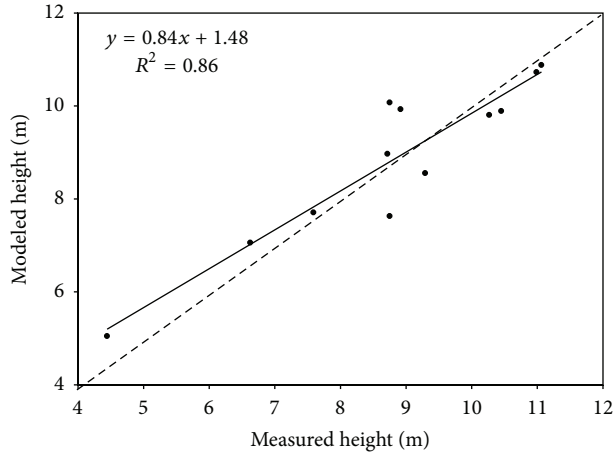

Figure 1: A comparison between measured and modeled mean tree height over the validation data subset.

4.2. Model Parameters and Comparisons with Measured Results. Both components of (1) had statistically significant predictive capability with almost equal positive magnitude of multipliers (slope = 0.8, $P < 0.01$ and slope = 0.6, $P < 0.05$ for COMP and SITE, resp.) showing that the variation of H_t was sufficiently explained by either measure. The overall regression's P value was 0.001, with $R^2 = 0.84$ and no recognized multicollinearity (VIF = 1.25). We suggest that the inclusion of the "age" parameter as one of the independent predictors (significant at $P < 0.004$ level as compared with $P = 0.4$ for ln(CCF)) could be speculated to be a reason for the higher significance of a COMP variable. In addition to the ecological meaning of such inclusion, in planted stands it provides a good explanation for the within-stand variation in tree sizes, because it is tightly related to stand density manipulations.

Figure 1 compares measured with predicted values of mean tree height for 12 CC classes over the validation dataset. It reveals high and significant correlation between the two ($R^2 = 0.86$; $P < 0.01$). Table 2 shows that both sets resulted in an identical average ($H_t = 9$ m) with a small standard deviation (STD) that was ~11% higher for the measured than for the predicted dataset (1.9 and 1.7 m, resp.), which highlights the higher intrinsic variability of the former.

Here it must be noted that though the effect of ln(CCF) was not statistically significant for the model represented by (2), excluding it from the calculation did not change the correlation level depicted in Figure 1, nor the resulting statistics (see below) in the specific case. Nevertheless, we decided to include it in the final model, as it is the only parameter that takes into account the "social status" of trees

Table 2: Comparison between measured and predicted values of mean tree height for twelve CC classes (each class represents an average of two plots) over the validation dataset. Each class contains two cases. Relative and absolute errors were calculated as RE = (|measured − modeled|)/measure and AE = |measured − modeled|, respectively.

CC class	COMP	SITE	Measured height (m)	Modeled height (m)	Relative Error	Absolute error (m)
<30	8.44	6.35	6.6	7.1	0.07	0.4
30–35	9.43	9.79	10.5	9.9	0.05	0.6
35–40	5.71	6.67	4.4	5.0	0.14	0.6
40–45	9.74	7.25	9.3	8.6	0.08	0.7
45–50	7.37	8.98	7.6	7.7	0.02	0.1
50–55	9.38	10.30	8.8	10.1	0.15	1.3
55–60	10.04	10.55	11.0	10.7	0.02	0.3
60–65	11.04	9.52	11.1	10.9	0.02	0.2
65–70	10.01	9.31	8.9	9.9	0.11	1.0
70–75	7.22	9.17	8.8	7.6	0.13	1.1
75–80	9.32	10.07	10.3	9.8	0.05	0.5
>80	9.96	7.89	8.7	9.0	0.03	0.3
AVG	**8.97**	**8.82**	**8.8**	**8.8**	**0.07**	**0.59**
STD	**1.53**	**1.43**	**1.9**	**1.8**	**0.05**	**0.39**
R^2	**0.2**		**0.86**			
P value	**0.15**		**<0.01**			
VIF	**1.25**					

Table 3: Comparison between measured and predicted values of mean tree height.

Plot	Measured height (m)	Predicted height (m)	Absolute error (m)
1	8.8	9.1	0.3
2	7.4	8.1	0.7
3	8.5	9.1	0.6
4	8.0	8.3	0.3
5	7.7	8.2	0.5
6	9.1	9.1	0
AVG	**8.3**	**8.7**	**0.4**
STD	**0.66**	**0.50**	**0.25**
R^2	**0.88**		
Slope	**0.71**		
Offset	**2.83**		
P value	**<0.01**		

within the plot, and including it seemed important from the silvicultural point of view.

Further analysis of the data is presented in Table 3. It highlights that for more than 75% of the classes the absolute error (AE = |measured − modeled|) was less than or equal to 1 m, whereas a higher deviation from the measured data was registered for the remaining 25% of the classes (i.e., two cases). Both groups, however, remained within the boundaries of the standard error for photogrammetric interpretation of aerial photography used by the Survey of Israel (i.e., 2 m, I. Sosnitsky, personal communication). The average AE was 0.6 m and was considered to be negligible. The average relative error (RE = |measured − modeled|/measured) was 7% ± 5%; it was smaller than 10% for 66.67% of classes and never exceeded 15%. Hence, based on a combination of high correlation coefficient (Figure 1) and the above statistics we deduced that the overall accuracy of the model could be considered adequate, demonstrating the validity of the linear approximation (1).

In light of the results presented in Table 2, the proposed model (1) was implemented for mapping mean tree height over the SSA on a per-pixel basis, as based on a multispectral satellite image. All variables required for the SITE term were assessed at 20 m spatial resolution DTM [29]. A 4 m spatial resolution IKONOS image was then aggregated to 20 m resolution, to make it comparable with DTM.

The FVC was calculated according to (4) with values of 0.13 and 0.75 used for $NDVI_{min}$ and $NDVI_{max}$, respectively [30]. This resulted in a map of the spatial distribution of FVC that ranged from 40% to 70% over the study area within the entire image, and averaged 51.5% ± 4% for the six training plots. This value corresponds to an average CC calculated from measured crown width of 50% ± 11%, with an average absolute error less than 10% ± 6%. The FVC was then used to calculate the CCF as discussed in details by Sprintsin et al. [17] and, consequently, the COMP term.

Figure 2 is a map of spatial distribution of mean tree height over 1 km^2. This map was then overlain with the vector layer of six 1000 m^2 plots. The mean H_t value for each plot was extracted with a Zonal Statistics procedure of the ERDAS Imagine software and then compared with ground-based measurements. Those comparisons, presented in Table 3, show high and significant linear correlation between the calculated and measured values (R^2 = 0.88; slope = 0.71; P < 0.01) indicating freedom from systematic error in

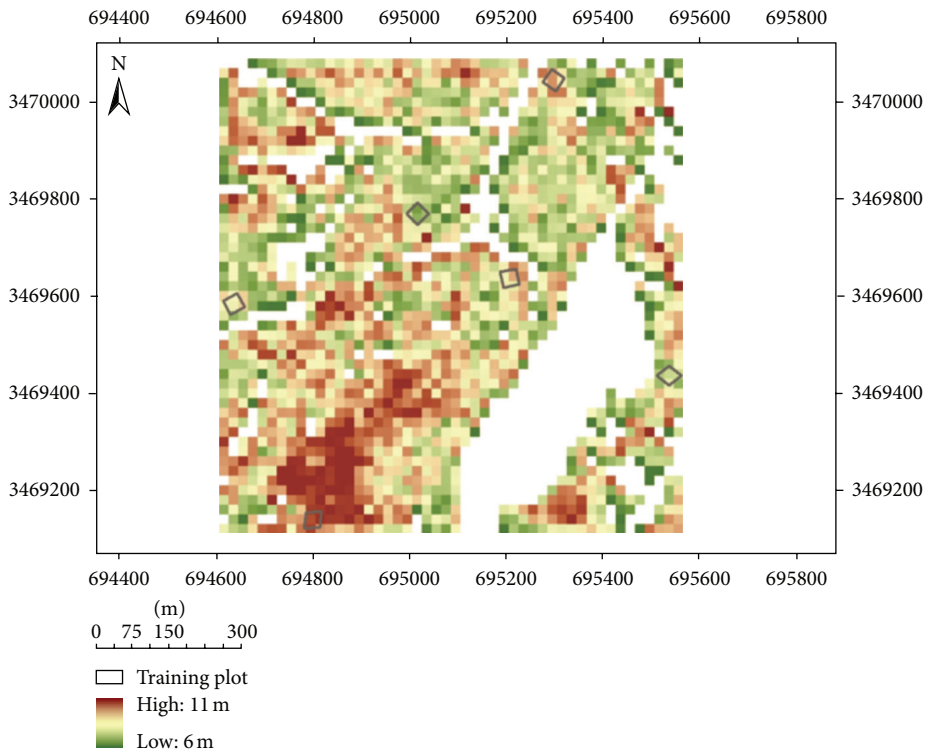

Figure 2: Spatial distribution of mean tree height over the specific study area. Note the location of training plots used in validation of the map accuracy (gray squares).

the calculations. It also shows that both sets were very comparable with regard to mean values (8.3 and 8.7 m for measured and modeled sets, resp.) and on a plot-to-plot basis, with an absolute error that never exceeded 0.7 m and had an average of 0.4 m, which was considered as negligible.

4.3. Practical Implementation of the Proposed Methodology. As was mentioned earlier in this paper (Section 1), accurate approximation of the mean tree height could benefit hydrometeorological studies for which detailed description of canopy structure is required in estimation of surface aerodynamic roughness properties and consequent assessment of water and energy balances. To test the accuracy of the proposed methodology, the measured and the calculated values of H_t for each CC class of the validation data subset (see Table 2) were used as an input for surface aerodynamic resistance (r_a) calculations [40]:

$$r_a = \frac{\ln\left((z-d)/z_0\right)}{k^2 u}, \quad (5)$$

in which z is the height of meteorological measurements (15 m for Yatir); d_c is the zero-plane displacement (m); z_0 is the roughness length (m), u is the wind speed (m s^{-1}), and k is von Karman's constant ($k = 0.41$). d_c and z_0 were taken as a fraction of tree height ($d_c = 0.78H_t$ and $z_0 = 0.075H_t$ after [41] for conifers). Wind speed was taken to be constant ($u = 2.7$ m s^{-1}), approximated from the tower-top (18 m height) measurements that were averaged for daylight hours over six consecutive years (2000–2006).

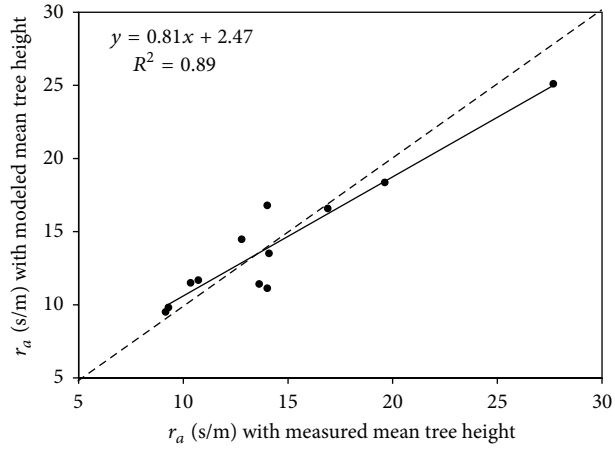

Figure 3: Comparison between aerodynamic resistance (r_a) calculated from field-measured values of mean tree height (H_t) and that calculated from mean tree height as estimated with the presented model (1)–(3).

Figure 3 compares resistance calculated from field-measured values of $H_t(r_{a,\text{meas}})$ with that based on estimated $H_t(r_{a,\text{mod}})$. A comparison between the two sets revealed almost equal values ($r_{a,\text{mod}} = 14.4 \pm 5.2$ s m^{-1}; $r_{a,\text{meas}} = 14.2 \pm 4.5$ s m^{-1}) and low relative error, averaging 10% ± 1%. The respective sets were highly correlated ($R^2 = 0.89$) and not significantly different from one another.

5. Discussion and Conclusions

One of the challenges currently faced by foresters is how to assess the spatial extent of standard forest characteristics. Remote-sensing methods, with their ability to cover large areas while entailing moderate costs, seem to offer a good answer to this challenge. Thus, it is important to be able to relate surface phenomena to spectral characteristics. However, as we mentioned above (Section 1), not every forest parameter has its own unique spectral response. For this reason, determining an optimal compromise between minimization of inputs and lowering spatial resolution should be a major task of remote sensing applications, and this was a major aim of the present study. This objective was achieved by adopting stand-level mean canopy cover—the only parameter that can be simply extracted from multispectral optical remote sensing imagery—as a proxy for other forest structural characteristics. Our approach determines the mean tree height of a forest stand by using a combination of landscape, stand, and canopy characteristics. Such a combination reflects the interactions among the varied factors that are responsible for tree growth and precisely describes the "social position" of an individual tree within a particular stand. Accurate estimation of the height of a vegetation layer, in turn, leads to a better determination of surface aerodynamic roughness properties and their spatial distribution, which could be easily and accurately derived from multispectral observations. These outputs can contribute to hydrometeorological studies and evaluation of the regional water and energy balance.

We should note, however, that the main challenge that one could face in applying the presented methodology in environments other than drylands is the proper estimation of CC from multispectral imagery. The main reason for this difficulty is the signal generated by understory vegetation (which is generally negligible in semiarid and arid regions) that could seriously contaminate the reflectance of a single pixel. In such cases, the number of end members of spectral mixture analysis model will be increased and an appropriate unmixing technique will be required [42]. Nevertheless, although it is technically possible to measure the crown projection area on remote sensing imagery, the actual maximum crown width cannot always be defined (even on aerial photographs) because of neighboring trees and overlapping crowns [43]. One important issue, therefore, is to examine the difficulties encountered in applying the proposed method in more complex terrain, mixed forests and milder climates that are characterized by more complex structures of vegetation layer.

The results presented here, however, indicate that the proposed combination of landscape and canopy characteristics can be exploited for mean tree height assessment on the regional scale in simply structured environments. The model presented here serves the need to estimate tree characteristics from their canopy extent; it helps to satisfy the requirement to reduce the need for fieldwork in single-tree-based forest inventories and to fill the knowledge gap caused by underrepresentation of the available applications in the current forestry literature.

Acknowledgment

The authors are grateful to the Israeli Forest Service (Keren Kayemet LeIsrael-Jewish National Fund) for the help with the field measurements.

References

[1] D. Sellier, Y. Brunet, and T. Fourcaud, "A numerical model of tree aerodynamic response to a turbulent airflow," *Forestry*, vol. 81, no. 3, pp. 279–297, 2008.

[2] G. Zagalikis, A. D. Cameron, and D. R. Miller, "The application of digital photogrammetry and image analysis techniques to derive tree and stand characteristics," *Canadian Journal of Forest Research*, vol. 35, no. 5, pp. 1224–1237, 2005.

[3] S. R. Cloude and K. P. Papathanassiou, "Polarimetric SAR interferometry," *IEEE Transactions on Geoscience and Remote Sensing*, vol. 36, no. 5, pp. 1551–1565, 1998.

[4] C. H. Hug and A. Wehr, "Detecting and identifying topographic objects in imaging laser altimetry data," *International Archives of Photogrammetry and Remote Sensing*, vol. 32, part 3-4W2, pp. 19–26, 1997.

[5] K. Kraus and W. Rieger, "Processing of laser scanning data for wooded areas," in *Photogrammetric Week 1999*, D. Fritsch and R. Spiller, Eds., pp. 221–231, Wichmann, Heidelberg, Germany, 1999.

[6] J. A. B. Rosette, P. R. J. North, and J. C. Suárez, "Vegetation height estimates for a mixed temperate forest using satellite laser altimetry," *International Journal of Remote Sensing*, vol. 29, no. 5, pp. 1475–1493, 2008.

[7] S. N. Coward and D. L. Williams, "Landsat and earth systems science: development of terrestrial monitoring," *Photogrammetric Engineering and Remote Sensing*, vol. 63, no. 7, pp. 887–900, 1997.

[8] M. A. Lefsky, W. B. Cohen, G. G. Parker, and D. J. Harding, "Lidar remote sensing for ecosystem studies," *BioScience*, vol. 52, no. 1, pp. 19–30, 2002.

[9] P. A. Zollner and K. J. Crane, "Influence of canopy closure and shrub coverage on travel along coarse woody debris by eastern chipmunks (*Tamias striatus*)," *American Midland Naturalist*, vol. 150, no. 1, pp. 151–157, 2003.

[10] F. Berger and F. Rey, "Mountain protection forests against natural hazards and risks: new french developments by integrating forests in risk zoning," *Natural Hazards*, vol. 33, no. 3, pp. 395–404, 2004.

[11] B. J. Choudhury, N. U. Ahmed, S. B. Idso, R. J. Reginato, and C. S. T. Daughtry, "Relations between evaporation coefficients and vegetation indices studied by model simulations," *Remote Sensing of Environment*, vol. 50, no. 1, pp. 1–17, 1994.

[12] J. Wang, P. M. Rich, K. P. Price, and W. D. Kettle, "Relations between NDVI and tree productivity in the central Great Plains," *International Journal of Remote Sensing*, vol. 25, no. 16, pp. 3127–3138, 2004.

[13] J. Jensen, *Introductory Digital Processing: A Remote Sensing Perspective*, Prentice-Hall, Englewood Cliffs, NJ, USA, 1996.

[14] C. J. Nichol, K. F. Huemmrich, T. A. Black et al., "Remote sensing of photosynthetic-light-use efficiency of boreal forest," *Agricultural and Forest Meteorology*, vol. 101, no. 2-3, pp. 131–142, 2000.

[15] M. F. Garbulsky, J. Peñuelas, D. Papale, and I. Filella, "Remote estimation of carbon dioxide uptake by a Mediterranean forest," *Global Change Biology*, vol. 14, no. 12, pp. 2860–2867, 2008.

[16] A. Goerner, M. Reichstein, and S. Rambal, "Tracking seasonal drought effects on ecosystem light use efficiency with satellite-based PRI in a Mediterranean forest," *Remote Sensing of Environment*, vol. 113, no. 5, pp. 1101–1111, 2009.

[17] M. Sprintsin, A. Karnieli, S. Sprintsin, S. Cohen, and P. Berliner, "Relationships between stand density and canopy structure in a dryland forest as estimated by ground-based measurements and multi-spectral spaceborne images," *Journal of Arid Environments*, vol. 73, no. 10, pp. 955–962, 2009.

[18] G. W. Koch, S. C. Stillet, G. M. Jennings, and S. D. Davis, "The limits to tree height," *Nature*, vol. 428, no. 6985, pp. 851–854, 2004.

[19] N. Liphschitz, O. Bonneh, and Z. Mendel, "Living stumps—circumstantial evidence for root grafting in *Pinus halepensis* and *P. brutia* plantations in Israel," *Israel Journal of Botany*, vol. 36, pp. 41–43, 1987.

[20] H. Hasenauer and R. A. Monserud, "A crown ratio model for Austrian Forests," *Forest Ecology and Management*, vol. 84, no. 1–3, pp. 49–60, 1996.

[21] S. Condés and H. Sterba, "Derivation of compatible crown width equations for some important tree species of Spain," *Forest Ecology and Management*, vol. 217, no. 2-3, pp. 203–218, 2005.

[22] L. E. Krajicek, K. A. Brinkman, and S. F. Gingrich, "Crown competition—a measure of density," *Forest Science*, vol. 7, pp. 35–42, 1961.

[23] T. E. Avery and H. E. Burkhart, *Forest Measurements*, McGraw-Hill, New York, NY, USA, 1994.

[24] D. M. Hyink and S. M. Zedaker, "Stand dynamics and the evaluation of forest decline," *Tree Physiology*, vol. 3, pp. 17–26, 1987.

[25] C. Deleuze, J. Herve, F. Colin, and L. Ribeyrolles, "Modelling crown shape of Picea abies: spacing effects," *Canadian Journal of Forest Research*, vol. 26, no. 11, pp. 1957–1966, 1996.

[26] A. Mäkelä and P. Vanninen, "Impacts of size and competition on tree form and distribution of aboveground biomass in Scots pine," *Canadian Journal of Forest Research*, vol. 28, no. 2, pp. 216–227, 1998.

[27] H. Ishii, J. P. Clement, and D. C. Shaw, "Branch growth and crown form in old coastal Douglas-fir," *Forest Ecology and Management*, vol. 131, no. 1–3, pp. 81–91, 2000.

[28] M. J. Ducey, "Predicting crown size and shape from simple stand variables," *Journal of Sustainable Forestry*, vol. 28, no. 1-2, pp. 5–21, 2009.

[29] J. K. Hall, "DTM project scheme of 1:50,000 topographic sheet mnemonics for Israel," *Geological Survey of Israel Current Research*, vol. 8, pp. 47–50, 1993.

[30] M. Sprintsin, A. Karnieli, P. Berliner, E. Rotenberg, D. Yakir, and S. Cohen, "The effect of spatial resolution on the accuracy of leaf area index estimation for a forest planted in the desert transition zone," *Remote Sensing of Environment*, vol. 109, no. 4, pp. 416–428, 2007.

[31] J. M. Grünzweig, T. Lin, E. Rotenberg, A. Schwartz, and D. Yakir, "Carbon sequestration in arid-land forest," *Global Change Biology*, vol. 9, no. 5, pp. 791–799, 2003.

[32] N. J. Crookstone and A. R. Stage, *Percent Canopy Cover and Stand Structure Statistics from the Forest Vegetation Simulator*, USDA Publication, 1999.

[33] Y. Tominaga, "Representative subset selection using genetic algorithms," *Chemometrics and Intelligent Laboratory Systems*, vol. 43, no. 1-2, pp. 157–163, 1998.

[34] A. Gusnanto, Y. Pawitan, J. Huang, and B. Lane, "Variable selection in random calibration of near-infrared instruments: ridge regression and partial least squares regression settings," *Journal of Chemometrics*, vol. 17, no. 3, pp. 174–185, 2003.

[35] L. D. Schroeder, D. L. Sjoquist, and P. E. Stephan, *Understanding Regression Analysis*, Sage Publications, Beverly Hills, Calif, USA, 1986.

[36] R. J. Freund, R. C. Littell, and L. Creighton, *Regression Using JMP*, SAS Institute, Cary, NC, USA, 2003.

[37] D. A. Belsley, E. Kuh, and R. E. Welsch, *Regression Diagnostics: Identifying Influential Data and Sources of Collinearity*, John Wiley & Sons, New York, NY, USA, 1980.

[38] R. D. Snee, "Some aspects of nonorthogonal data analysis—part I: developing prediction equations," *Journal of Quality Technology*, vol. 5, no. 2, pp. 67–79, 1973.

[39] E. F. Vermote, D. Tanré, J. L. Deuzé, M. Herman, and J. Morcrette, "Second simulation of the satellite signal in the solar spectrum, 6s: an overview," *IEEE Transactions on Geoscience and Remote Sensing*, vol. 35, no. 3, pp. 675–686, 1997.

[40] W. Brutsaert, *Evaporation into the Atmosphere: Theory, History, and Applications*, Kluwer Academic Publishers, Dordrecht, The Netherlands, 1982.

[41] H. G. Jones, *Plant and Microclimate*, Cambridge University Press, Cambridge, UK, 2nd edition, 1992.

[42] J. Pisek and J. M. Chen, "Mapping forest background reflectivit over North America with Multi-angle Imaging SpectroRadiometer (MISR) data," *Remote Sensing of Environment*, vol. 113, no. 11, pp. 2412–2423, 2009.

[43] J. Kalliovirta and T. Tokola, "Functions for estimating stem diameter and tree age using tree height, crown width and existing stand database information," *Silva Fennica*, vol. 39, no. 2, pp. 227–248, 2005.